Author(s): Puska, Martti J. & Sob, M. & Brauer, G. & Korhonen, T.

Title: First-principles calculation of positron lifetimes and affinities in perfect and imperfect transition-metal carbides and nitrides

Year: 1994

Version: Final published version

Please cite the original version:

Puska, Martti J. & Sob, M. & Brauer, G. & Korhonen, T. 1994. First-principles calculation of positron lifetimes and affinities in perfect and imperfect transition-metal carbides and nitrides. Physical Review B. Volume 49, Issue 16. 10947-10957. ISSN 1550-235X (electronic). DOI: 10.1103/physrevb.49.10947.

First-principles calculation of positron lifetimes and affinities in perfect and imperfect transition-metal carbides and nitrides

M. J. Puska
Laboratory of Physics, Helsinki University of Technology, SF-02150 Espoo, Finland

M. Šob
Institute of Physical Metallurgy, Academy of Sciences of the Czech Republic, Žižkova 22, CZ-616 62 Brno, Czech Republic

G. Brauer
Positron Group of the Technical University of Dresden at Research Centre Rossendorf Inc., P.O. Box 510119, D-01314 Dresden, Federal Republic of Germany

T. Korhonen
Laboratory of Physics, Helsinki University of Technology, SF-02150 Espoo, Finland
(Received 28 October 1993)

First-principles electronic structure and positron-state calculations for transition-metal carbides and nitrides are performed. Perfect NaCl structures as well as structures with metal or carbon/nitrogen vacancies are considered. The positron affinities and lifetimes are determined. The trends are discussed and the results are compared with recent positron lifetime measurements for group-IV and -V refractory metal carbides. The present analysis suggests, contradictory to an earlier interpretation, that positrons are trapped and annihilated at both carbon and metal vacancies. The concentration of metal vacancies detected by positron annihilation methods is probably very low, below the sensitivity limit of other experimental methods.

I. INTRODUCTION

Refractory metal carbides and nitrides exhibit interesting physical properties, e.g., high melting points, extreme hardness, and relatively high superconducting transition temperatures. These make them attractive for both theoretical investigations and technological applications.[1–4] Many of their desirable characteristics are critically influenced by the presence of vacancies, which occur mostly on the nonmetal sublattice. Experimental evidence shows that, e.g., in the rocksalt ($B1$) modification of these compounds, up to 30% of the lattice sites may be vacant (i.e., up to 60% of the nonmetal sublattice). Thus, the presence of vacancies in refractory metal carbides and nitrides seems to be an intrinsic property of these compounds.[3,4]

Positron annihilation spectroscopy (PAS) is a sensitive technique for studying lattice defects with electron density less than average, the vacancies in particular. In pure metals PAS yields very precise values of vacancy formation enthalpies, and the process of positron trapping at point defects in pure metallic elements is more or less well understood.[5,6]

The behavior of point defects in alloys and intermetallic compounds is somewhat more complicated than in pure metals. First, several types of vacancies and interstitials may exist, some of them with peculiar properties. In many processes, different types of defects may compete, thus complicating the underlying physical mechanisms. In this case it is important to be able to detect these various defect types and to resolve their role in the processes studied.

Due to the larger variety of defects in alloys and intermetallics, the interpretation of the PAS experimental data is more difficult than in pure metals. In most cases, a thorough theoretical analysis is indispensable in order to determine how various types of defects are reflected in the PAS data and to draw some quantitative conclusions. Although the relation of positrons and vacancies in concentrated alloys has already been discussed in several publications (see, e.g., Refs. 7–9), one usually does not perform first-principles electronic structure calculations of positron properties in defects as, for example, in Ref. 10. Nevertheless, employing such calculations is generally the only way to understand the experimental PAS data in more complicated systems and to get a correct description of the defect properties.

In principle, vacancies may occur on both metal and nonmetal sublattices in refractory metal carbides and nitrides. However, most experimental results indicate that nonmetal vacancies are the predominant defects in these compounds, although vacancies on both sublattices have been reported, especially in (presumably metastable) superstoichiometric (i.e., nonmetal excess) compounds (see, e.g., Ref. 11 and the references therein). These experiments are usually performed by x-ray diffraction and pycnometry and their sensitivity may be estimated as not better than ± 0.005 in the resulting vacancy concentration.[12] Thus, if the concentration of vacancies on the metallic sublattice is less than 0.005, they will not be detected by the above-mentioned methods.

Positrons are sensitive to monovacancies in the concentration range 10^{-6}–10^{-3}, at least in pure metals. If the

concentration of vacancies is higher than about 10^{-3}, all positrons are trapped and annihilated in vacancies (saturation trapping). In this case, the corresponding PAS characteristics yield information not about the electronic structure of the bulk material, but about the features of the vacancies themselves.

In alloys and intermetallics the near environment of different types of vacancies may carry different net charges. As in the case of semiconductors[10] more negatively charged defects are expected to attract positrons more strongly. Therefore, preferential annihilation at some kinds of defects may take place, whereas some other types of defects are not detected at all.

Vacancy-free refractory metal carbides and nitrides exhibit a very high electronic density. The corresponding positron lifetime may be estimated to be about 100 ps; this is lower than the values found for most transition metals. Recent PAS measurements of Rempel *et al.*[13] yield values of 155–176 ps in refractory metal carbides, which were interpreted in terms of predominant positron annihilation with metal valence electrons, taking into account the presence of carbon vacancies even in nominally stoichiometric samples. It is one of the principal goals of this paper to find out, with the help of first-principles theoretical analysis, which types of vacancies affect the positrons in those materials, and to gain a deeper understanding of the experimental results.

In addition to the refractory (group-IV and -V) metal carbides and nitrides, which exist in the $B1$ structure, we have extended our calculations along the $3d$ transition-metal series up to Fe in order to see the trends exhibited by various quantities more clearly. It should be possible to generalize the main conclusions drawn for the $B1$-structure carbides and nitrides to the other structures as well.

Another important quantity which may be used in the analysis of the PAS data is the positron affinity. In a material with carbide or nitride precipitates, the difference in positron affinity between the precipitate and the matrix determines whether the precipitates are attractive or repulsive for the positron and, therefore, if they may be detected by PAS or not. Whether such a case occurs or not has been discussed in neutron-irradiated pressure vessel steels, and the present results are highly desirable to understand the PAS data obtained in those materials.[14,15] Let us remember that until recently positron affinities were calculated for elemental metals only.[16] Here we show that such calculations are tractable also for perfect and imperfect compounds.

The paper is organized as follows: in Sec. II the details of the calculation of electronic structure, positron affinity, and lifetime are given. Section III describes the theoretical results and their comparison with available experimental data. The electronic structures and positron characteristics are thoroughly discussed as well. Conclusions are presented in the closing Sec. IV.

II. COMPUTATIONAL METHOD

Our self-consistent electronic structure calculations as well as the determination of the positron states are based on density-functional theory within the local-density approximation (LDA).[17,18] In the LDA the effective potential for the electrons is written in the form

$$v_{\text{eff}}(\mathbf{r}) = \phi(\mathbf{r}) + v_{\text{xc}}(n(\mathbf{r})), \tag{1}$$

where $\phi(\mathbf{r})$ is the Coulomb potential due to the nuclei and electron charge density and v_{xc} is the LDA exchange-correlation potential,[19] which depends on the electron density $n(\mathbf{r})$. The effective potential determines, via one-electron wave functions, the electron density in turn. The ensuing problem has to be solved self-consistently. The one-electron eigenvalues give the electronic band structure, the most important parameter of which, for the present application, is the Fermi level.

The potential affecting the positron is constructed also in the LDA as

$$V_+(\mathbf{r}) = -\phi(\mathbf{r}) + V_{\text{corr}}(n(\mathbf{r})), \tag{2}$$

where ϕ is the Coulomb potential as in Eq. (1), and V_{corr} is the correlation potential describing the energy lowering due to the electron pileup near the positron. The correlation potential V_{corr} is treated within the LDA based on many-body calculations for a delocalized positron in a homogeneous electron gas.[18]

We calculate the self-consistent electronic structures of different carbides and nitrides using the linear-muffin-tin-orbital method (LMTO) within the atomic-spheres approximation (ASA).[20] For a given compound, the radii of the metal atom and the carbon or nitrogen atom spheres are chosen to be equal. The core electron wave functions in the solid state are frozen to be the free-atom functions. The valence electron wave functions are determined scalar relativistically using partial waves up to $l = 2$ for the transition-metal spheres and up to $l = 1$ for the carbon or nitrogen spheres. The spheres are arranged into the NaCl lattice structure and lattice constants are determined by minimizing the total energy.

In the calculations for the NaCl-structure carbides and nitrides with vacancies a supercell with eight atomic sites (Fig. 1) is used. For the lattice constants the values optimized for perfect crystals are employed. The atoms neighboring the vacancies are not allowed to relax from their perfect lattice positions. The positron states are calculated also in the supercell geometry using the same numerical methods.

In the LMTO-ASA method the potentials and energy levels are given with respect to the so-called *crystal zero* level, which is defined as the zero of the Coulomb potential due to the nuclei and the electron density of the infinite solid. In the ASA the lattice is divided into spheres centered around nuclei. The spheres fill the whole space and the electron density and the potentials are approximated to be spherical inside these spheres. Therefore the calculation of the Coulomb potential and the determination of the crystal zero is easy. For example, in the case of fcc and bcc metals, for which all the spheres are identical neutral Wigner-Seitz spheres, the Coulomb potential due to every sphere vanishes just outside its surface. The position of the Fermi level relative to the crystal zero defines the electron chemical potential μ_-. For positrons,

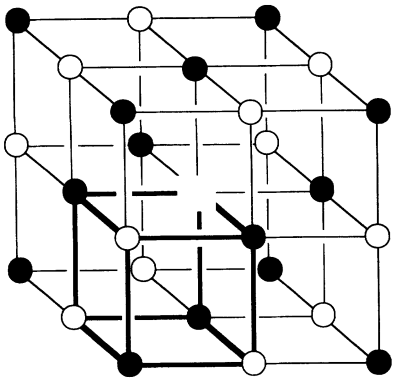

FIG. 1. NaCl structure with a vacancy. For a vacancy in the metal (nonmetal) sublattice the white and black circles denote the metal (nonmetal) and nonmetal (metal) atoms, respectively. The supercell used in the calculations consists of eight sites forming a regular small cube. The sites are occupied by four black and three white circles and one site is vacant.

the position of the bottom (at $\mathbf{k} = \mathbf{0}$) of the lowest energy band relative to the crystal zero gives the positron chemical potential μ_+.

The positron affinity A_+ is defined as the sum

$$A_+ = \mu_- + \mu_+. \tag{3}$$

The importance of the positron affinity is that the difference of the positron energies between different materials in contact is the difference in their positron affinities.[16] Positrons have the lowest absolute energy level in the material which has the lowest (negative) positron affinity. Moreover, the positron affinity is an important quantity in surface physics studied by slow-positron beam techniques. For example, the positron affinity is related to the measured positronium formation energy and to the positron work function. For the relations between positron energetics and the affinity in the case of solid surfaces, see Ref. 16.

The positron lifetime τ is calculated from the electron and positron densities within the LDA.[21–23] In the LDA, the total positron annihilation rate $\lambda = 1/\tau$ reads as

$$\lambda = \int d\mathbf{r}\; n_+(\mathbf{r})\Gamma(n_-(\mathbf{r})), \tag{4}$$

where $n_+(\mathbf{r})$ is the positron density and $\Gamma(n_-)$ is the positron annihilation rate in a homogeneous electron gas with density n_-.[18] We underline that the present LDA calculations give first-principles results for both the positron affinities and the lifetimes, i.e., there are no adjustable parameters in our calculations.

III. RESULTS AND DISCUSSION

A. Electronic structures

The calculated NaCl-structure lattice constants for the transition-metal carbides and nitrides are given in Table I. The results for TiC, VC, TiN, and VN are in good agreement with previous LMTO-ASA calculations.[24] For the carbides and also for the nitrides the lattice constants decrease along the 3*d* series. However, they increase sharply when going downward in the Periodic Ta-

TABLE I. Calculated properties of the NaCl-structure transition-metal carbides and nitrides. The perfect lattices (MX, M = transition metal, X = C or N) as well as lattices containing metal (M_3X_4) and carbon or nitrogen (M_4X_3) vacancies are considered. The results for bcc Fe and orthorhombic Fe_3C with the experimental lattice constants are shown, too. For the carbides and nitrides the NaCl-structure lattice constants a are optimized for the perfect lattices. The experimental lattice constants (Ref. 39) are given in parentheses; for Fe_3C the lattice parameters from Ref. 34 were used. μ_- and μ_+ denote the electron and positron chemical potentials, respectively. A_+ and τ are the positron affinity [Eq. (3)] and lifetime, respectively. The positron affinities and lifetimes differ slightly from the previously published values (Ref. 14) due to a better self-consistency and more accurate determination of the positron potential in the present calculations.

Material	a (a_o)	μ_- (eV)	μ_+ (eV)	A_+ (eV)	τ (ps)
TiC	8.060 (8.175)	+2.0	−3.8	−1.8	98
Ti_3C_4		−0.9	−6.7	−7.6	161
Ti_4C_3		+1.9	−5.1	−3.2	124
VC	7.802 (7.881)	+3.3	−3.5	−0.2	89
V_3C_4		+0.3	−6.8	−6.6	149
V_4C_3		+2.2	−5.4	−3.2	117
CrC	7.641	+3.1	−3.3	−0.1	84
Cr_3C_4		+0.6	−6.6	−6.0	141
Cr_4C_3		+2.4	−5.2	−2.9	112
MnC	7.544	+2.8	−3.2	−0.4	82
Mn_3C_4		+0.8	−6.5	−5.7	136
Mn_4C_3		+2.2	−5.1	−2.9	109
FeC	7.415	+2.4	−3.0	−0.5	78
Fe_3C_4		+0.8	−6.2	−5.4	129
Fe_4C_3		+1.8	−5.1	−3.3	106
ZrC	8.880 (8.878)	+0.7	−3.7	−3.0	114
Zr_3C_4		−1.6	−5.9	−7.5	196
Zr_4C_3		+1.0	−5.4	−4.4	148
NbC	8.620 (8.447)	+1.9	−2.3	−0.4	105
Nb_3C_4		−0.2	−4.8	−5.0	181
Nb_4C_3		+1.2	−4.8	−3.5	138
HfC	8.690 (8.766)	+1.4	−3.1	−1.6	105
Hf_3C_4		−1.8	−5.9	−7.7	185
Hf_4C_3		+1.7	−5.1	−3.4	137
TaC	8.566 (8.420)	+3.0	−2.9	+0.1	99
Ta_3C_4		−0.5	−6.3	−6.8	177
Ta_4C_3		+1.8	−5.6	−3.8	130
TiN	8.143 (8.013)	+5.0	−3.8	+1.2	100
Ti_3N_4		+0.5	−7.4	−6.9	159
Ti_4N_3		+3.5	−6.0	−2.6	143
VN	7.968 (7.826)	+4.5	−3.5	+1.0	94
V_3N_4		+0.8	−7.1	−6.2	154
V_4N_3		+3.4	−5.6	−2.2	138
CrN	7.830	+3.8	−3.5	+0.3	89
Cr_3N_4		+0.6	−7.0	−6.5	147
Cr_4N_3		+3.4	−5.5	−2.1	123
Fe	5.406	−1.3	−3.1	−4.4	99
Fe_3C		+1.9	−2.5	−0.6	91

ble from the 3*d* series to the 4*d* series and then they decrease slightly between the 4*d* and 5*d* series. These trends reflect the changes in the localization of the uppermost *d* wave functions. The calculated lattice constants are compared with the experimental values in cases where the NaCl structure is stable. The theoretical lattice constants calculated in the LDA are expected to be smaller than the experimental ones, but in our results this is not true for ZrC, NbC, TaC, TiN, and VN. Moreover, the experimental trend that the lattice constant for a nitride is slightly smaller than that for the corresponding carbide is not obeyed in the calculated results (Table I). The reason for these small discrepancies is most probably the ASA, which cannot describe open lattice structures accurately enough without empty spheres. The NaCl structure is on the borderline between dense (fcc, bcc) and open (diamond) lattice structures.[24]

As an example of the calculated electronic structures we show in Fig. 2 the density of states (DOS) for TiC. Again, the present results agree very well with previous KKR (Korringa-Kohn-Rostoker)[25] and LMTO-ASA[24,26] calculations. In the total DOS the first structure on the left is due to mainly *s*-type states of carbon. The broad structure just below the Fermi level corresponds to the hybridized C *p* and Ti *d* bands. Above the Fermi level the main contribution to the DOS comes from the Ti *d* bands. The DOS's for the other NaCl-structure carbides and nitrides are very similar to that for TiC. Thus, the relative position of the the Fermi level for the different compounds depends primarily on the number of valence electrons. For the group-IV refractory metal carbides TiC, ZrC, and HfC the Fermi level is near a deep minimum of the DOS, whereas for the other carbides and nitrides considered in this work the Fermi level is situated in the high-DOS region of the metal *d* bands. The position of the Fermi level relative to the DOS is reflected also in the behavior of the electron chemical potential, i.e., in the position of the Fermi level relative to the crystal zero. According to Table I the electron chemical potential for carbides rises strongly from TiC to VC and then decreases slowly toward FeC. The nitrides TiN, VN, and CrN, which we have studied, are in the region of decreasing electron chemical potential (the number of valence electrons in TiN is the same as in VC). In the case of transition-metal carbides, going down within group IV or group V first lowers the electron chemical potential between the 3*d* and 4*d* series, but increases it between the 4*d* and 5*d* series. This behavior reflects again changes in the localization of the *d* wave functions or in the bandwidths.

The effects due to introduction of carbon or nitrogen vacancies agree with previous notions[24,25,27–29] [the main reason for the minor differences between our DOS's and those in the above papers is probably the use of a larger number of *k* points (84 in the irreducible Brillouin zone) in our calculations]. The reduction in the number of valence electrons has a tendency to lower the electron chemical potential. As seen in Fig. 3, in Ti_4C_3 the carbon vacancies have only small effects on the positions of the different band edges. But the prominent features are the induced peaks in the DOS at the minimum between the carbon-*p*–metal-*d* hybridized bands and the metal *d* bands (directly at the Fermi energy in the case of Ti_4C_3). These peaks have the metal *d* character and they are due to the breaking of the carbon-metal bonds.[24] Because for

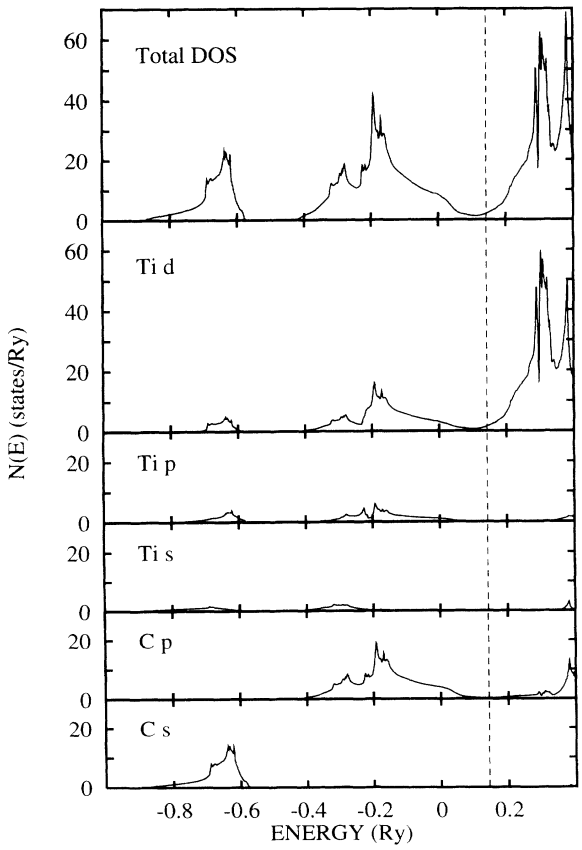

FIG. 2. Total density of states for TiC and its different components. The Fermi level is denoted by a dashed line.

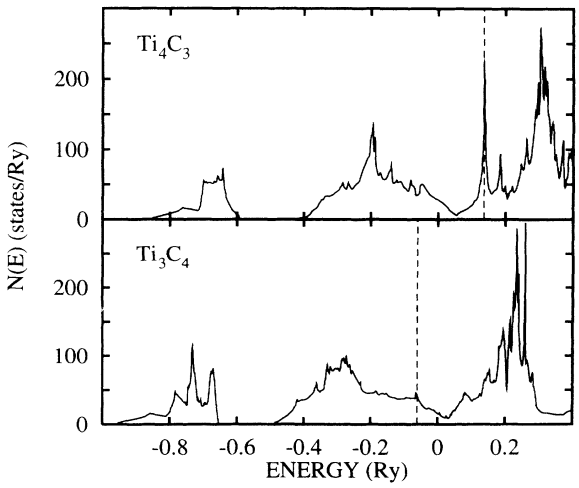

FIG. 3. Total density of states for the vacancy lattices Ti_4C_3 and Ti_3C_4. The Fermi level is denoted by a dashed line.

the group-IV carbides the Fermi level is around the minimum in the DOS and thus at the same region as the induced peaks, the Fermi level is pinned by these peaks. As a result, the electron chemical potential decreases only slightly in TiC, and in ZrC and HfC it even increases due to the introduction of carbon vacancies. In the cases of the other carbides and nitrides studied, the vacancy-induced peaks are at lower energies relative to the Fermi level and the carbon or nitrogen vacancies decrease the value of the electron chemical potential.

As discussed in Refs. 29 and 30, some of the nonmetal vacancy peaks may be due to the long-range ordering of the vacancies in the calculated structures. Therefore the number, intensity, and position of the vacancy-induced peaks may be different for disordered systems or for isolated vacancies. However, the position of the Fermi level and the value of the DOS at the Fermi level will hardly influence the calculated positron lifetime, as it is determined by the total electron density [Eq. (4)]. There might be some minor changes in the calculated values of positron affinities, but, as our results show, they cannot influence the physical conclusions drawn in the present paper. Thus, as far as the calculated positron lifetimes and affinities are concerned, they may be only slightly changed due to vacancy ordering. As we are primarily interested in isolated vacancies, we have made convergence tests of positron annihilation characteristics with respect to the size of the elementary cell. The results of those tests are described in Sec. III C.

As we can see from Fig. 3, the metal vacancies do not induce new prominent peaks. The Fermi level is lowered with respect to the perfect crystal both due to the overall shift of the bands and due to the reduction in the number of valence electrons.

The above details of the electronic structures are important for the positron properties as well, namely, the behavior of the Fermi level makes a large contribution to the trends in the positron affinity (as will be discussed below). Moreover, the fact that these systems are metallic guarantees that the position of the electron chemical potential is well defined, in contrast to the case of semiconductors or insulators, in which its actual position in the band gap is determined by the experimental conditions. Finally, the metallic character means that formulas for positron correlation energy and for the annihilation rate that are based on the free-electron-gas model are expected to be valid.

B. Positron states

The values of the positron chemical potential calculated by the LMTO-ASA method are given in Table I. For perfect lattices the positron chemical potential varies only slowly from one system to another. It decreases when the open volume experienced by the positron increases. The introduction of metal vacancies lowers the positron chemical potential on the average by 3 eV, whereas the lowering by the smaller-sized carbon or nitrogen vacancies is about 2 eV, only.

In order to visualize the positron states and to test the results for the positron lifetimes we have also applied the superimposed-atom method[31] for the present systems. Here the electron density is non-self-consistent (it is given by the superposition of the free-atom densities), but the benefit of this approach relative to the LMTO-ASA is that the real three-dimensional geometry is treated correctly (the potentials and charge densities are not assumed spherical). The positron densities in the perfect TiC lattice as well as in the lattices Ti_3C_4 and Ti_4C_3 containing Ti and C vacancies, respectively, are shown in Fig. 4. The plane of the figure is the (110) cut of the supercells used in the LMTO-ASA vacancy calculations (Fig. 1). In the perfect lattice the positron wave function has its maxima at the interstitial regions and vanishes toward the Ti or C nuclei. In the case of the Ti vacancy the positron density is clearly localized around the vacant site, whereas for the C vacancy the positron exhibits a stronger diffusion toward the super-

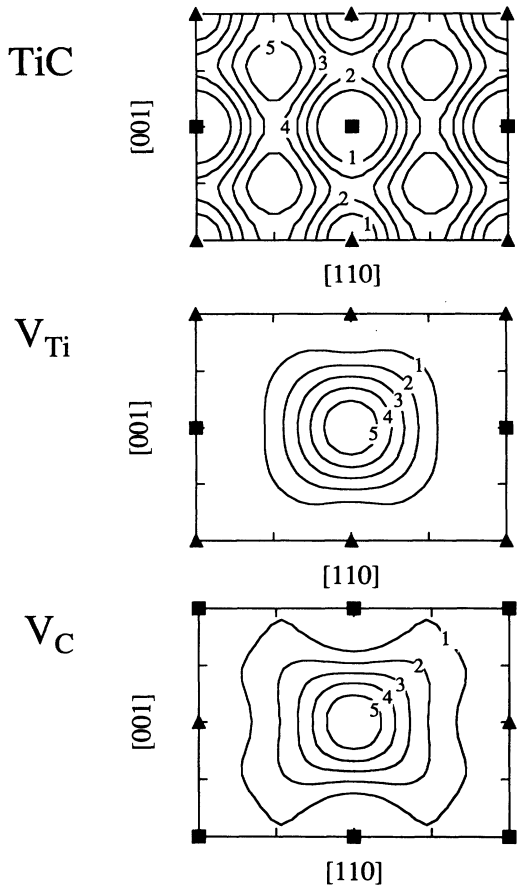

FIG. 4. Positron density in perfect TiC and the vacancy lattices Ti_4C_3 and Ti_3C_4. The panels show the regions of the (110) planes limited by the borders of the supercells used. For each panel the contour spacing is one-sixth of the maximum value. Normalizing the positron densities so that there is one positron inside the supercell, the maximum positron densities are $0.0038a_0^{-3}$, $0.0139a_0^{-3}$, and $0.0099a_0^{-3}$ for Ti_4C_4, Ti_3C_4, and Ti_4C_3, respectively. The black triangles and squares denote the positions of the carbon and titanium nuclei, respectively.

cell boundaries. This means that the effects due to the finite supercell size are expected to be stronger for the carbon or nitrogen vacancies than for the metal vacancies. However, the localization of the positron density in the vacancies seen in Fig. 4 means that the positron results, for example the lifetimes obtained, may be considered also as results for isolated vacancies.

C. Positron lifetimes and affinities

The calculated positron lifetimes for the different transition-metal carbides and nitrides are given in Table I, for both undefected and defected lattices. The lifetimes are shown also in Fig. 5 as a function of the unit cell volume. For a given type of system, i.e., for perfect bulk lattices and the two types of defected lattices, the positron lifetime depends rather linearly on the unit cell volume and thus on the open volume available for positrons. However, for $4d$ and $5d$ carbides the lifetimes are at lower values than the extrapolation from the data for the $3d$ carbides would indicate. The carbon vacancy lifetimes in $3d$ carbides are about 1.35 times longer than the bulk lifetimes, whereas the corresponding ratio for the metal vacancy lifetimes is about 1.67. For the $4d$ and $5d$ carbides the difference in lifetimes between the metal and carbon vacancies increases slightly. For comparison, typical vacancy-bulk lifetime ratios for metals are about 1.6 and for semiconductors less than about 1.3. It is also interesting to note that the lifetime difference between the two types of vacancies is smaller in nitrides than in carbides. This is in accordance with the larger number of valence electrons of the nitrogen atom compared to the carbon atom.

The calculated positron lifetimes in perfect transition-metal carbides and nitrides are low, substantially lower than the calculated[21–23] or experimental[32] lifetimes in the corresponding pure metals. These low values reflect their high atomic and electronic densities. For example, we can consider TiC as a fcc Ti metal with the octahedral sites occupied by carbon impurities. The lattice constant of $8.06a_0$ (or the experimental one $8.175a_0$) is only slightly larger than $7.81a_0$ which corresponds to the experimental atomic volume of Ti metal (a_0 is the Bohr radius, equal to the atomic unit). According to the atomic-superposition calculations, the increase of the Ti lattice constant from $7.81a_0$ to $8.06a_0$ ($8.175a_0$) increases the positron lifetime from 150 ps to 164 ps (170 ps). In the fcc lattice the positron density has maxima at the octahedral sites. However, the introduction of the octahedral carbon fills in these sites and removes the positron into the interstitial sites of the NaCl lattice. The overlap of electron and positron wave functions is then much larger and, as a result, the positron lifetime in TiC reduces to 98 ps.

The differences between the metal and carbon or nitrogen vacancies deserve further comment. Let us consider again TiC as an example; the situation in the other carbides and nitrides is similar. Table II shows the valence electron and positron distributions among the different atomic spheres in the perfect and vacancy TiC lattices (the Ti and C sphere radii are equal). The partial positron annihilation rates with valence and core electrons within different spheres are given, too. The positron distributions are normalized to unity in each case, whereas the sum of the valence electron contributions gives the total number of valence electrons in the

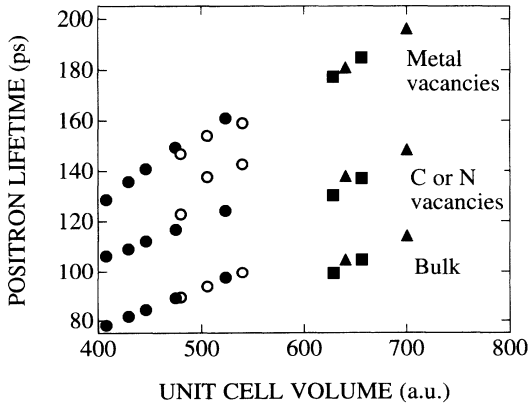

FIG. 5. Positron lifetimes for the perfect transition-metal carbide or nitride lattices and for the lattices with metal and carbon or nitrogen vacancies as a function of the conventional unit cell volume [(lattice constant)^3]. The different $3d$ transition-metal carbides and nitrides are denoted by black and open circles, respectively. The $4d$ and $5d$ transition-metal carbides are denoted by black squares and triangles, respectively.

TABLE II. Electron and positron distributions and partial positron annihilation rates in perfect TiC and in TiC containing Ti (Ti_3C_4) or C (Ti_4C_3) vacancies. The distributions and the partial annihilation rates are given in the ASA for Ti and C spheres and in the case of vacancy lattices also for the (empty) vacancy spheres (E). All the sphere radii are equal. M is the number of spheres of the given type in the supercell. For a given sphere, N_- and N_+ are the total valence electron and positron charges, respectively, and λ_c and λ_v are the partial annihilation rates with core and valence electrons, respectively. In the case of supercells with a vacancy there are four different types of spheres (see Fig. 1). The rows for Ti_3C_4 (Ti_4C_3) are ordered so that the uppermost row corresponds to the vacancy sphere E and the second row to the three C (Ti) spheres neighboring the E sphere. The third and fourth rows correspond to the three Ti (C) spheres and one C (Ti) sphere, which are the second- and third-nearest neighbors of the E sphere, respectively.

Material	Sphere	M	N_-	N_+	λ_c (ns^{-1})	λ_v (ns^{-1})
TiC	Ti	4	2.922	0.111	0.506	0.656
	C	4	5.078	0.139	0.021	1.382
Ti_3C_4	E	1	0.912	0.512	0.000	1.884
	C	3	4.459	0.116	0.013	0.982
	Ti	3	2.889	0.037	0.154	0.220
	C	1	5.048	0.024	0.003	0.222
Ti_4C_3	E	1	1.433	0.381	0.000	1.859
	Ti	3	2.767	0.103	0.461	0.566
	C	3	5.109	0.084	0.012	0.826
	Ti	1	2.938	0.058	0.255	0.345

supercell. In the perfect lattice, there is a charge transfer of about one electron from a Ti sphere to a C sphere. Because of this and the smaller ionic core size of carbon the positron resides more in the C spheres and, therefore, the annihilation takes place preferably in the C spheres rather than in the Ti spheres.

Due to the charge transfer described above, metal vacancies may be considered as more negative environments (they are surrounded by negative C spheres) whereas carbon vacancies are more positive. Indeed, according to Table II within the supercell for the titanium vacancy the net charge of the vacancy sphere and of six of its neighboring C spheres is about $-3.7|e|$ (e is the electron charge). Similarly, the carbon vacancy sphere and its six neighboring Ti spheres have a net charge of about $+6.0|e|$. Therefore, the positron density is better localized inside the titanium vacancy than in the carbon vacancy (see Table II). This difference is clear also from the positron densities in Fig. 4. Because of the good localization, the annihilation at the titanium vacancy happens mainly in the vacancy sphere and in the six neighboring C spheres (see Table II), whereas in the case of the carbon vacancy there are relatively large contributions to the annihilation rate from the more distant spheres, too. As a consequence, the positron lifetime for the titanium vacancy is 37 ps longer than for the carbon vacancy.

The positron affinities calculated according to Eq. (3) are given in Table I. For the perfect lattices the affinities are higher than those for most elemental metals.[16] This reflects again high electronic densities in carbides and nitrides. For the materials with carbon or nitrogen vacancies the positron affinities are about 3 eV lower than the affinities for perfect crystals. In the case of group-IV transition-metal carbides this lowering is smaller due to the pinning of the Fermi level. The decrease of the positron affinity due to metal vacancies is stronger, on the average about 6 eV. The high positron affinities for the perfect carbide and nitride lattices suggest that these materials could be used as effective moderators in the slow-positron beam technique. The problem may, however, be the difficulty of producing high-quality single crystals with a low vacancy concentration.

In Table I we show data for bcc Fe, too. This is because the transition-metal carbides are thought to be the irradiation-induced precipitates in reactor pressure vessel steels. Precipitates formed by neutron irradiation have already been studied by PAS.[33] According to Table I the carbide precipitates in Fe could trap positrons and be observable only if they contain metal vacancies because only in that case is their affinity for the positron lower (more negative) than the iron affinity. In order to approach closer to the reality in steels we have also performed calculations for the compound Fe_3C, cementite. This is an existing carbide, in contrast to the FeC with the NaCl structure discussed above. Fe_3C has an orthorhombic unit cell with 16 atoms. In the calculations we have used the measured lattice constants.[34] The band structure and the density of states obtained agree well with those calculated recently by Häglund *et al.*[35] using also the LMTO-ASA method. The positron annihilation results for Fe_3C are shown at the bottom of Table I. It is seen that the Fermi level in Fe_3C is quite high relative to bcc Fe. This fact, in addition to the increase of the positron chemical potential, decreases the absolute value of the positron affinity and makes positron trapping at perfect Fe_3C precipitates in steels impossible. Due to a large computation cost, we have not performed calculations for vacancies in Fe_3C, but we expect that their properties, with respect to positron states, will be qualitatively similar to those for FeC. The consequences of the present positron affinity data in the interpretation of the PAS results for irradiated reactor pressure vessel steels are discussed in another context.[14,15]

The positron binding energy to one isolated vacancy can be estimated from the supercell calculations as follows. In principle, one should have one vacancy in the supercell and increase the size of the supercell until the electron and positron energy levels do not change anymore. The positron binding energy to the vacancy would be the asymptotic value of the positron affinity difference between the vacancy system and the perfect bulk material. Because the electron chemical potential approaches the electron chemical potential for the perfect material when the supercell size increases, the positron binding energy would be obtained also from the positron chemical potential difference. When the supercell increases the value of the positron chemical potential for the vacancy system is mainly affected by the development of the electrostatic potential near the vacancy. The effects due to overlapping of positron wave functions from the neighboring shells vanish rapidly because of the localization of the positron wave function. The net effect is, however, that the difference in the positron affinity converges more rapidly than the difference in the positron chemical potential. This is due to the fact that the changes in electron and positron chemical potentials partly cancel each other.

We have tested these ideas by performing calculations for TiC with larger supercells. In the case of a C vacancy the electron chemical potential is pinned by the peaks in the DOS and therefore its changes are small. The changes in the positron chemical potential and consequently in the positron affinities are small as well. For example, if the size of the supercell is increased from Ti_4C_3 to Ti_8C_7, the chemical potentials and the positron affinity change less than ≈ 0.2 eV. The positron binding energies calculated from the positron chemical potentials and from the positron affinities (Table I) agree then with the same accuracy. The case of the Ti vacancy is more interesting. The positron binding energies calculated from the positron chemical potentials and from the positron affinities for different supercells are shown in Table III. The binding energy calculated from the affinity difference increases slowly as a function of the supercell size whereas that calculated from the chemical potential difference exhibits a much stronger dependence. The agreement between the two approaches improves remarkably if the size of the supercell increases. Note that the distance from a vacancy to its nearest periodic image is the same for Ti_3C_4, Ti_7C_8, and $Ti_{15}C_{16}$ but the number of nearest images decreases from 6 to 2 in the given order. This leads to the nearly linear behavior of the binding energies seen

TABLE III. Positron binding energy E_b at the Ti vacancy in TiC estimated from calculations with different supercells. The binding energy is determined as the difference between the positron chemical potentials ($\Delta\mu_+$) or the positron affinities (ΔA_+) for the supercell containing a vacancy and for the perfect bulk lattice. The energies are in eV.

Supercell	$E_b(\Delta\mu_+)$	$E_b(\Delta A_+)$
Ti_3C_4	2.9	5.8
Ti_7C_8	3.9	5.9
$Ti_{15}C_{16}$	4.6	6.0
$Ti_{31}C_{32}$	5.3	6.1

in Table III. For $Ti_{31}C_{32}$ the distance between the nearest vacancies has increased by a factor of 2 and we expect that the binding energy calculated as the affinity difference will converge by better then 0.1 eV. These results show that the positron affinity is a very useful quantity in the determination of the positron binding energies, too.

According to the positron affinities given in Table I, the positron binding energies to the metal vacancies are larger than to the carbon vacancies. This is consistent with the differences in positron localization in these vacancies (Fig. 4 and Table II) and with the fact that the positron lifetimes are longer at the metal vacancies than at the carbon or nitrogen vacancies.

The results of the atomic-superposition calculations for the positron lifetimes and binding energies to vacancies in TiC and VC are given in Table IV. Results for the other carbides and nitrides are similar. The supercells used in these calculations contain 8 and 7 atoms for the perfect and vacancy lattices, respectively. It can be seen that the atomic-superposition method gives slightly longer lifetimes for the bulk and for the carbon vacancies than LMTO-ASA. In the case of metal vacancies, at which the positron wave functions are well localized, the values from atomic-superposition and LMTO-ASA calculations are in very good agreement. The positron binding energies at vacancies in the atomic-superposition method are calculated as the difference of the positron energy eigenvalues between the perfect bulk lattice and the lattice containing a vacancy. The positron binding energies given in Table IV can be compared with those obtained from the positron affinity differences in Table I. According to this comparison, the atomic superposition seems to underestimate the binding energy approximately by 1 eV in most cases. The discrepancies in the lifetime and binding energies arise from the different geometrical approximations and from the differences in the self-consistency of the electron densities.[23] The conclusion is, however, that the atomic-superposition calculations confirm well the trends found in the LMTO-ASA results; the lifetime values are even in very good agreement. The atomic-superposition method allows us to test the effects of the supercell size on the positron lifetimes at vacancies. The use of a supercell with 63 atoms gives positron lifetimes of 174 ps and 126 ps for Ti and C vacancies, respectively. The increase of the size of the supercell seems to have opposite effects on the positron lifetime for these vacancies, compared to the LMTO-ASA values. Nevertheless, we may summarize that there is a good overall agreement between both methods, and small numerical differences do not influence the physical conclusions drawn.

TABLE IV. Positron lifetimes τ and binding energies E_b at vacancies obtained by the atomic-superposition method.

Material	τ (ps)	E_b (eV)
TiC	107	
Ti_3C_4	160	4.8
Ti_4C_3	131	1.7
VC	98	
V_3C_4	147	4.8
V_4C_3	121	1.9

D. Comparison with positron lifetime measurements

Let us compare the present calculated positron lifetimes with recent measurements of Rempel *et al.*[13] for group-IV and group-V transition-metal carbides in Table V. The theoretical and experimental positron lifetimes for the corresponding transition metals are shown for comparison, too. These theoretical values were obtained previously[23] by the same methods as the present carbide results. The calculated positron lifetimes for the

TABLE V. Comparison of the theoretical and experimental positron lifetimes for the NaCl-structure transition-metal carbides. The perfect lattices (MC, M = transition metal) as well as lattices containing metal (M_3C_4) and carbon (M_4C_3) vacancies are considered. The lifetimes calculated (Ref. 23) for the transition metals are shown for comparison. τ_{theo} is the calculated lifetime and τ_{expt} denotes the experimental lifetime. For a given carbide, τ_v is the mean value of the theoretical positron lifetime corresponding to the metal and carbon vacancies.

Material	τ_{theo} (ps)	τ_v (ps)	τ_{expt} (ps)
TiC	98	143	160[a] (TiC)
Ti_3C_4	161		
Ti_4C_3	124		
Ti	146[b]		147[a]
ZrC	114	172	176[a] ($ZrC_{0.98}$)
Zr_3C_4	196		
Zr_4C_3	148		
Zr	159[b]		165[a]
NbC	105	159	161[a] (NbC)
Nb_3C_4	181		151[a] ($NbC_{0.72}$)
Nb_4C_3	138		
Nb	122[b]		119[a]
HfC	105	161	173[a] (HfC)
Hf_3C_4	185		
Hf_4C_3	137		
Hf	149[b]		174[a]
TaC	99	154	155[a] ($TaC_{0.99}$)
Ta_3C_4	177		
Ta_4C_3	130		
Ta	117[b]		116[a]

[a]Reference 13.
[b]Reference 23.

transition metals correspond very well to the measured values in most cases. This gives us confidence in the theoretical methods, especially the LDA, for predicting the positron lifetimes.

It may be seen from Table V that the experimental lifetimes are much longer than the lifetimes calculated here for perfect carbide lattices. It is interesting to note that, for example, the measured lifetime of 160 ps for TiC would correspond to the TiC lattice from which all the carbon atoms are removed and the remaining fcc Ti lattice is not allowed to relax (see the discussion in Sec. III C). As a matter of fact, Rempel *et al.*[13] arrived at a similar result using simpler arguments. However, their conclusion was that, in the refractory metal carbides, positrons annihilate mainly with metal valence electrons and that the contribution of the carbon electrons to the annihilation is vanishingly small. According to the present calculations annihilation with carbon electrons is important (see Table II) and the experimental lifetimes correspond rather to configurations with vacancies.

A more detailed comparison of the theoretical and experimental results shows that, with surprisingly good accuracy, the measured lifetimes correspond to the average of the lifetimes calculated in the structures with metal and carbon vacancies (τ_v in Table V). Only in the case of TiC does the measured lifetime seem to correspond well to the lifetime for a titanium vacancy. On the basis of these results, it seems that in TiC positrons annihilate mostly at the Ti vacancies, whereas in the other carbides the annihilation takes place at both metal and carbon vacancies.

Rempel *et al.*[13] found that the positron lifetime in NbC_y continually decreases from 161 ps to 151 ps when the carbon content is decreased from $y = 1.00$ to $y = 0.72$. They concluded that this is due to the increase of annihilation with metal electrons. According to the present results and our interpretation, the decrease of the positron lifetime reflects the fact that the positron annihilation at metal vacancies becomes less pronounced in the sample with a lower carbon content, in favor of annihilation at carbon vacancies.

There is also another argument in favor of positron annihilation at vacancies and not in the bulk. Manuel[36] has measured two-dimensional angular correlation positron annihilation spectra of NbC, which were fully isotropic. He interpreted his results as an indication of positron trapping at vacancies, as no modulation due to bulk electronic momentum density was present.[37]

Thus, on the basis of the above discussion, it seems that a decisive role of vacancies in positron annihilation in refractory metal carbides is very likely. Except in the case of TiC, both metal and carbon vacancies should be involved in these materials and, therefore, one would expect at least two different lifetime components. Unfortunately, the resolution and statistics of the measurements presented by Rempel *et al.*[13] did not allow a reliable decomposition.[12] That is why only average positron lifetimes were given. However, these average lifetimes fully correspond to our interpretation. Future measurements with a better resolution power and higher statistics should verify or disprove it.

One could also think that the experimental lifetimes correspond to the carbon vacancies only, in which case the too-low theoretical values would be due to the omission of the lattice relaxation around the vacancy. However, using the atomic-superposition method, we have estimated that, for instance, in TiC this model requires an outward (breathing) relaxation of the Ti atoms neighboring the C vacancy, which is about 10% of the nearest-neighbor atom distance. Such a large relaxation is improbable for dense carbides or nitrides. Carbon vacancy agglomerates could also possibly cause the relatively long measured positron lifetimes, although their existence is quite improbable in well annealed stoichiometric samples. We have studied this idea by performing atomic-superposition calculations for clusters of two, three, and four vacancies in TiC and NbC. In these calculations the supercells are obtained from the 64-atom bulk supercell by removing carbon atoms which are nearest neighbors to each others and keeping the metal atoms in their ideal lattice positions. The results are shown in Table VI. The increase in the positron lifetime is rather slow. Only three-dimensional vacancy clusters of at least four atoms give lifetimes which are close to the measured ones. In this case the annihilation takes place mainly with electrons from the metal atoms, and the situation resembles the above-discussed annihilation in a transition metal with increased lattice constant. (From the calculational point of view it is interesting to note that the positron binding energies at carbon vacancies given in Table VI for the large supercell are smaller than those for the smaller supercell given in Table IV. This reflects the finite positron band dispersion in the case of the smaller supercell.)

However, the possibility of carbon or nitrogen vacancy clusters must be considered as highly hypothetic in refractory metal carbides and nitrides. Carbon vacancies form ordered superstructures[3,4] and, therefore, their in-

TABLE VI. Positron lifetimes τ and binding energies E_b at carbon vacancy clusters in TiC and NbC. N is the number of vacancies forming the vacancy cluster. The results are obtained by the atomic-superposition method using supercells with $64 - N$ atoms. $N = \infty$ denotes the results for the bare fcc metal lattice with the lattice constant of the corresponding metal carbide.

Material	N	τ (ps)	E_b (eV)
TiC	0	107	
	1	126	0.7
	2	140	1.7
	3	147	2.4
	4	153	2.9
	∞	164	4.2
NbC	0	114	
	1	133	0.7
	2	145	1.5
	3	151	2.1
	4	156	2.5
	∞	165	3.5

teraction is repulsive (see also Ref. 38, where the effective cluster interactions for carbon vacancies in substoichiometric VC have been computed). Thus, the formation of three-dimensional carbon or nitrogen vacancy clusters is not favored. The nonmetal vacancies can be closer together only if their concentration is high enough. However, this was not the case of the samples used in Ref. 13, which were nearly stoichiometric. The existence of carbon vacancy clusters in those samples is, therefore, highly improbable.[12]

Thus, the comparison of our theoretical positron lifetimes with the measured ones strongly indicates the existence of metal vacancies in the samples. Their concentration may, however, be small in comparison with that of the carbon vacancies, if the positron has a much larger preference to annihilate at the former, i.e., if the positron trapping coefficient for the metal vacancies is much larger than for the carbon vacancies. As a matter of fact, this is probably the case, because the binding energies to the metal vacancies are larger than to the carbon vacancies and the trapping coefficient (for the electron-hole excitation process relevant here) increases as the binding energy increases.[40] Moreover, it is known that positron trapping at positively charged vacancies in semiconductors practically vanishes due to the repulsive Coulomb barrier, although there is a bound positron state at the vacancy.[10] According to Table II, the nearest environment of the carbon vacancy has a net positive charge whereas that of the metal vacancy has a net negative charge. The net positive charge may lead to a repulsive Coulomb barrier near the carbon vacancy, although due to the screening this barrier has, in contrast to the case of a semiconductor, a finite range. Thus, the different characters of the total charge densities for the carbon and metal vacancies can lead to preferential positron trapping into the metal vacancies prior to the carbon vacancies.

Independent (i.e., nonpositron) evidence for the existence of metal vacancies in $B1$-type refractory metal carbides and nitrides is rare. Metal vacancies in ZrN were reported in Refs. 41, 42, and 43. Straumanis[43] found a considerably high metal vacancy concentration also in TiN and HfN (up to 6.31% in nominally stoichiometric HfN). A high structural defect concentration on the Ti sublattice in TiN was revealed in Refs. 44 and 45. Ehrlich[44] shows very nicely the decrease of the vacancy concentration on both metal and nonmetal sublattices in the series TiO–TiN–TiC, the defect concentration in TiC being zero within the experimental error limit. Thus, in refractory metal nitrides the existence of metal vacancies has been independently proved; in carbides they may exist as well according to these measurements, but in a small amount. From comparison of our calculations with the experimental results[13] we are not able to estimate the metal vacancy concentration in refractory metal carbides either. It will probably be lower than 0.005, the estimated sensitivity limit of the pycnometric and x-ray diffraction methods.[12,44] Further investigations in this direction would be desirable.

The only PAS results for refractory metal nitrides we are aware of have been published by Brunner and Perry.[11] They measured the positron lifetime spectra in TiN and HfN thin films. These data are hard to compare with our calculations because, in our opinion, these films and their interface with the substrate are not sufficiently well characterized.

IV. CONCLUSIONS

We have performed first-principles electronic structure and positron-state calculations for transition-metal carbides and nitrides. The quantities studied are the positron affinity and lifetime. For perfect carbide or nitride lattices the positron affinities are high and the lifetimes are short in comparison with the values for the corresponding transition metals. This result reflects the very high atomic and electronic density of the transition-metal carbides and nitrides. For lattices with metal or carbon/nitrogen vacancies the positron affinities are lower and the positron lifetimes longer than for the perfect lattices. The changes are larger for lattices with metal vacancies.

Comparison of the calculated positron lifetimes with recent measurements[13] for group-IV and group-V refractory metal carbides suggests that even in the highly stoichiometric systems positrons annihilate mainly at vacancies. Our results indicate that positrons are trapped and annihilated also at metal vacancies, the existence of which is difficult to see by other experimental methods. We suppose, on the basis of the self-consistent electronic structures, that the positron trapping coefficient is much larger for the metal vacancies than for the carbon vacancies. This makes the metal vacancies visible in PAS experiments, although their concentration will probably be lower than 0.005.

The theoretical values of positron lifetimes for refractory metal nitrides could not be compared with measurements because of lack of experimental data. In this sense, our results can be considered as predictions and should motivate positron annihilation experiments on these important materials.

The positron affinities calculated in this work are important parameters if used in the interpretation of positron annihilation results for materials containing carbide or nitride precipitates. A discussion about irradiation-induced precipitates in reactor vessel steels, which might consist of carbides and/or nitrides, is published elsewhere.[14,15]

ACKNOWLEDGMENTS

The authors wish to thank Dr. A. A. Rempel for stimulating discussions and Dr. A. Manuel for information about his two-dimensional angular correlation positron annihilation measurements on NbC.

[1] L. E. Toth, *Transition Metal Carbides and Nitrides* (Academic Press, New York, 1971).
[2] K. Schwarz, Crit. Rev. Solid State Mater. Sci. **13**, 211 (1987).
[3] A. I. Gusev, Phys. Status Solidi B **163**, 17 (1991); A. I. Gusev and A. A. Rempel, Phys. Status Solidi A **135**, 15 (1993).
[4] A. A. Rempel, *Ordering Effects in Non-Stoichiometric Interstitial Compounds* (Nauka, Ural Division, Ekaterinburg, 1992) (in Russian).
[5] For general reviews, see, e.g., *Positrons in Solids*, edited by P. Hautojärvi (Springer-Verlag, Berlin, 1979); *Positron Solid State Physics*, edited by W. Brandt and A. Dupasquier (North-Holland, Amsterdam, 1983).
[6] R. M. Nieminen, in *Positron Solid State Physics* (Ref. 5).
[7] S. M. Kim, in *Vacancies and Intersitials in Metals and Alloys*, Vols. 15–18 of Materials Science Forum, edited by C. Abromeit and H. Wollenberger (Trans Tech, Aedermannsdorf, 1987), pp. 1257, 1323.
[8] *Positron Annihilation*, edited by L. Dorikens-VanPraet, M. Dorikens, and D. Segers (World Scientific, Singapore, 1989).
[9] *Positron Annihilation*, Vols. 105–110 of Materials Science Forum, edited by Z. Kajcsos and C. Szeles (Trans Tech, Aedermannsdorf, 1992).
[10] M. J. Puska, C. Corbel, and R. M. Nieminen, Phys. Rev. B **41**, 9980 (1990).
[11] J. Brunner and A. J. Perry, Thin Solid Films **153**, 103 (1987).
[12] A. A. Rempel (private communication).
[13] A. A. Rempel, M. Forster, and H.-E. Schaefer, J. Phys. Condens. Matter **5**, 261 (1993); for a more detailed presentation, see A. A. Rempel, M. Forster, and H.-E. Schaefer, Dokl. Akad. Nauk SSSR **326**, 91 (1992) [Sov. Phys. Dokl. **39**, 484 (1992)].
[14] G. Brauer, M. Šob, and M. Puska, in *Positron Annihilation* (Ref. 9), p. 611. This paper is a preliminary report of the results presented in Ref. 15. The values of positron affinities and lifetimes differ slightly from those in Ref. 15 because of a better self-consistency and more accurate positron potential in the more recent calculations (Ref. 15).
[15] G. Brauer, M. J. Puska, T. Korhonen, and M. Šob (unpublished).
[16] M. J. Puska, P. Lanki, and R. M. Nieminen, J. Phys. Condens. Matter **1**, 6081 (1989).
[17] For a recent review, see R. O. Jones and O. Gunnarsson, Rev. Mod. Phys, **61**, 689 (1989).
[18] E. Boroński and R. M. Nieminen, Phys. Rev. B **34**, 3820 (1986).
[19] D. M. Ceperley and B. J. Alder, Phys. Rev. Lett. **45**, 566 (1980); we use their local exchange-correlation functional as parametrized by J. Perdew and A. Zunger, Phys. Rev. B **23**, 5048 (1981).
[20] For a recent review, see O. K. Andersen, O. Jepsen, and M. Šob, in *Electronic Band Structure and Its Applications*, edited by M. Yussouff (Springer-Verlag, Heidelberg, 1987), p. 1.
[21] K. O. Jensen, J. Phys. Condens. Matter **1**, 10 595 (1989).
[22] S. Daniuk, M. Šob, and A. Rubaszek, Phys. Rev. B **43**, 2580 (1991).
[23] M. J. Puska, J. Phys. Condens. Matter **3**, 3455 (1991).
[24] V. P. Zhukov, V. A. Gubanov, O. Jepsen, N. E. Christensen, and O. K. Andersen, J. Phys. Chem. Solids **49**, 841 (1988).
[25] P. Marksteiner, P. Weinberger, A. Neckel, R. Zeller, and P. H. Dederichs, Phys. Rev. B **33**, 812 (1986).
[26] J. Häglund, G. Grimvall, T. Jarlborg, and A. Fernández Guillermet, Phys. Rev. B **43**, 14 400 (1991).
[27] A. L. Ivanovsky, V. I. Anisimov, D. L. Novikov, A. I. Liechtenstein, and V. A. Gubanov, J. Phys. Chem. Solids **49**, 465 (1988).
[28] J. Redinger, R. Eibler, P. Herzig, A. Neckel, R. Podloucky, and E. Wimmer, J. Phys. Chem. Solids **46**, 383 (1985).
[29] P. Herzig, J. Redinger, R. Eibler, and A. Neckel, J. Solid State Chem. **70**, 281 (1987).
[30] A. Neckel, in *The Physics and Chemistry of Carbides, Nitrides and Borides*, edited by R. Freer (Kluwer Academic Publishers, Dordrecht, 1990), p. 485.
[31] M. J. Puska and R. M. Nieminen, J. Phys. F **13**, 333 (1983).
[32] A. Seeger, F. Banhart, and W. Bauer, in *Positron Annihilation* (Ref. 8), p. 275; A. Seeger and F. Banhart, Phys. Status Solidi A **102**, 171 (1987).
[33] G. Brauer, L. Liszkay, B. Molnar, and R. Krause, Nucl. Eng. Des. **127**, 47 (1991).
[34] R. W. G. Wyckoff, *Crystal Structures* (John Wiley and Sons, New York, 1964), Vol. 2.
[35] J. Häglund, G. Grimvall, and T. Jarlborg, Phys. Rev. B **44**, 2914 (1991).
[36] A. Manuel (private communication).
[37] A. Alam, J. H. Kaiser, P. A. Walters, R. L. Waspe, and R. N. West, in *Positron Annihilation*, edited by P. G. Coleman, S. C. Sharma, and L. M. Diana (North-Holland, Amsterdam, 1982), p. 331.
[38] V. Ozoliņš and J. Häglund, Phys. Rev. B **48**, 5069 (1993).
[39] The experimental lattice constants for carbides are those given in Ref. 13, for VC in Ref. 24, for TiN in A. N. Christiansen, Acta Chem. Scand. A **32**, 87 (1978), and for VN in B. R. Zhao, L. Chen, and H. L. Luc, Phys. Rev. B **29**, 6198 (1984).
[40] R. M. Nieminen and J. Laakkonen, Appl. Phys. **20**, 181 (1979).
[41] R. Juza, A. Gabel, H. Rabenau, and W. Klose, Z. Anorg. Allg. Chemie **329**, 136 (1964).
[42] M. E. Straumanis, C. A. Faunce, and W. J. James, Inorg. Chem. **5**, 2027 (1966).
[43] M. E. Straumanis, in *Anisotropy in Single-Crystal Refractory Compounds*, edited by F. W. Vahldiek and S. A. Mersol (Plenum Press, New York, 1968), p. 121.
[44] P. Ehrlich, Z. Anorg. Chem. **259**, 1 (1949).
[45] W. H. B. Hoondert, W. Th. M. Buters, B. J. Thijsse, and A. van den Beukel, Nucl. Instrum. Methods Phys. Res. B **59/60**, 1340 (1991).